Ultramicroscopy 116 (2012) 73–76

Contents lists available at SciVerse ScienceDirect

Ultramicroscopy

journal homepage: www.elsevier.com/locate/ultramic

The Young-Feynman two-slits experiment with single electrons: Build-up of the interference pattern and arrival-time distribution using a fast-readout pixel detector

Stefano Frabboni [a,b], Alessandro Gabrielli [c,d], Gian Carlo Gazzadi [b], Filippo Giorgi [c,d], Giorgio Matteucci [c], Giulio Pozzi [c,*], Nicola Semprini Cesari [c,d], Mauro Villa [c,d], Antonio Zoccoli [c,d]

[a] Department of Physics, University of Modena and Reggio Emilia, Via G. Campi 213/a, 41125 Modena, Italy
[b] CNR-Institute of Nanoscience-S3, Via G. Campi 213/a, 41125 Modena, Italy
[c] Department of Physics, University of Bologna, Viale B. Pichat 6/2, 40127 Bologna, Italy
[d] INFN, Viale B. Pichat 6/2, 40127 Bologna, Italy

ARTICLE INFO

Article history:
Received 20 July 2011
Received in revised form
22 March 2012
Accepted 23 March 2012
Available online 1 April 2012

Keywords:
Matter waves
Foundations of quantum mechanics
Measurement theory
Coherence in electron scattering
Microelectronics

ABSTRACT

The two-slits experiment for single electrons has been carried out by inserting in a conventional transmission electron microscope a thick sample with two nano-slits fabricated by Focused Ion Beam technique and a fast recording system able to measure the electron arrival-time. The detector, designed for experiments in future colliders, is based on a custom CMOS chip equipped with a fast readout chain able to manage up to 10^6 frames per second. In this way, high statistic samples of single electron events can be collected within a time interval short enough to measure the distribution of the electron arrival-times and to observe the build-up of the interference pattern.

1. Introduction

One of the most impressive experiments to investigate the wave behaviour of material particles is the single electron two-slits interference, an arrangement, adopted by Bohr and Einstein to develop their considerations on quantum mechanics foundations, widely quoted as Young-Feynman set-up [1]. Up to now, the superposition of electron waves has been demonstrated in a variety of arrangements, among which the Möllenstedt–Düker electron biprism [2,3] has been the most successful (see [4,5] for reviews covering the old and recent literature, respectively).

Nevertheless, the most striking part of the experiment, i.e. the build-up of two-beams interference pattern by single electrons arriving on the final screen, has never been observed with a two-slits set-up [6,7] but only with an electron biprism [4,5,8,9].

Recently, by using modern nanotechnology tools, two- [10] and multiple-slits [11] diffraction and interference experiments have been realized by means of a conventional transmission electron microscope (TEM) used as a versatile optical bench, instead of a dedicated instrument as done in the first experiments [6,7]. These experiments raised the interest of INFN researchers, which were developing CMOS detectors [12,13] for experiment in future colliders [14–17] so that we decided to join our forces in order to realize the original Young-Feynman set-up, whose pedagogical value and impact is of the utmost importance [18,19].

It should be pointed out that this experiment, with respect to the one carried out with the electron biprism, has the following advantages: (i) electrons do not interact with the electric field of the biprism and (ii) the images are Fraunhofer diffraction patterns, whose interpretation is much simpler than the Fresnel images of the biprism, where the effect of the electric field is overlapped to the diffraction due to the biprism edges [4,5].

In the present work, we present the first results obtained regarding the two-slits Young-Feynman experiment with electrons, where the final viewing screen of a commercial TEM has been replaced by our fast recording system, designed for collider experiments, which fortunately proved also sensitive to electrons. It has thus been possible to record the build-up of high statistic single electron interference patterns and to measure the time distribution of electron arrivals.

2. The experimental set-up

The slits were fabricated by using the technique of Focused Ion Beam (FIB) milling a gold layer about 250 nm thick deposited

* Corresponding author.
E-mail address: giulio.pozzi@unibo.it (G. Pozzi).

0304-3991/$ - see front matter © 2012 Elsevier B.V. All rights reserved.
http://dx.doi.org/10.1016/j.ultramic.2012.03.017

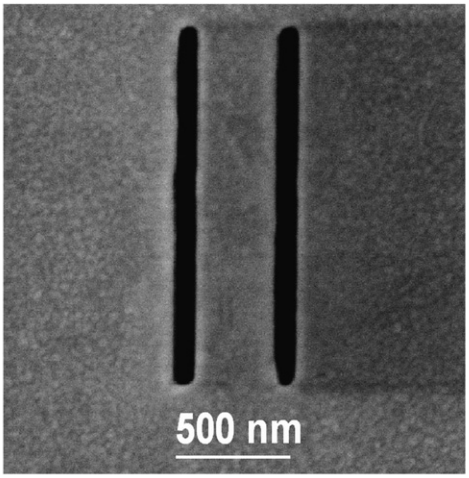

Fig. 1. Slits image obtained by scanning electron microscope (SEM).

by flash evaporation on a commercial copper grid coated with a carbon film. FIB milling was performed with a dual beam apparatus (FEI Strata *DB*235*M*), which combines a 30 keV-Ga$^+$ FIB with a thermal field emission scanning electron microscope (SEM), having spatial resolutions of 6 nm and 2 nm, respectively. The system is particularly versatile for nanoscale machining as it allows real time control of the work in progress by high-resolution SEM imaging.

To open the slits, a 10 pA beam, corresponding to an ion beam spot-size of about 10 nm, was scanned over $100 \times 1500\ \mathrm{nm}^2$ rectangular patterns, 440 nm spaced, 5 s for each pattern. The passage through the gold–carbon bilayer was monitored by detecting the change in brightness of the ion-induced secondary electron emission. The width of each slit is about 95 nm, and their separation and length are 430 nm and 1550 nm, respectively, as measured from the darker region visible inside the secondary electrons SEM image reported in Fig. 1.

Interference experiments were carried out with a Philips EM400T transmission electron microscope, equipped with a hair-pin filament source operating at 60 keV (de Broglie wavelength $\lambda = 4.86$ pm). Owing to the small diffraction angles (of the order of 10^{-5} rad) associated with the slits separation, interference patterns must be observed in the so-called low-angle diffraction mode. In this electro-optical set-up, the condenser lenses must be excited at their maximum strength in order to reach the necessary lateral coherence and the objective lens is weakly excited in order to project the interference pattern onto the selected area aperture plane. By varying the excitation of the remaining lenses of the electron microscope, an enlargement of this pattern onto the detector is obtained. Therefore, the microscope works as a diffraction camera having camera length which can be increased up to several hundred meters. The best operating conditions were chosen by calibrating the camera length by means of a carbon grating (spacing 463 nm).

The sensor used to detect electrons is a custom silicon chip called Apsel4D, composed of a matrix of 128×32 pixels – monolithic active pixel sensors (MAPS) – developed in 0.13 μm CMOS technology and equipped with a fast digital readout. Each pixel ($50 \times 50\ \mu\mathrm{m}^2$ area) can provide a hit/not-hit information tagged with a time-stamp label. The sensor chip has been designed for the vertex detector's innermost layers of the next generation of particle physics experiments. These chips have been designed having in mind high efficiency ($>90\%$), high reliability, low budget material and high particle rates (up to 100 MHz/cm^2). In order to satisfy these requirements, the Apsel4D chip has been developed as a very fast and efficient Application Specific Integrated Circuit (ASIC). The pixels do not provide information on the detected charge, and this minimizes the output data stream.

During functioning, an external periodic signal, called BCO (Bunch Cross-Over) for historical reasons, is used to tag the time hit pixels. At each BCO signal the matrix is swept in search for hit pixels that are read out from the matrix area. Read pixels become immediately sensitive to external signals minimizing in this way dead time. Outside the matrix area a sparsifier and buffering logic that identify the hit pixels provides also the space and time association to hits and sends the data outside with a rate up to 21 bits per clock cycle. The chip has been designed so that, on average, only few pixels are hit during a BCO period, and only those hit pixels are actually sent out to a data acquisition system (DAC). This is in contrast with a standard CCD-based imaging system [20], where all pixels are actually read out.

The actual read frequency and time-stamping capabilities depends on the read clock and the BCO clock frequencies. The chip has been designed with peak performances of a 100 MHz read clock and a 10 MHz BCO clock frequencies. The chip has been studied extensively on proton and pion beam tests at CERN [14,16], where spatial resolutions compatible with $50/\sqrt{12}\ \mu\mathrm{m}$ have been measured and confirmed. Runs performed with 2.5 MHz BCO clock frequencies (400 ns period) have demonstrated the capability of the chip to stand continuously the 10^6 fps although, in the experimental conditions of the present data taking, a much more conservative BCO frequency of 6.25 kHz has been used (165 μs period).

3. Results

In order to obtain single electrons travelling through the electron microscope column, the intensity of the beam current is selected to satisfy two conflicting requirements. On one hand, it must be high enough to collect high statistic samples within a time interval that guarantees a stable operativeness of the interferometer. On the other hand, in order to obtain the needed lateral coherence of the illumination, the condenser lens system is strongly excited thus resulting in a decreasing of the beam current. Once established the optimal working conditions of the electron microscope, the frame rate has been chosen in order to contain, below the percent level, the fraction of frames with electron multiplicity higher than one.

A pictorial view of the stack of few frames collected in a typical run is shown in Fig. 2. Starting from the bottom, the first frame

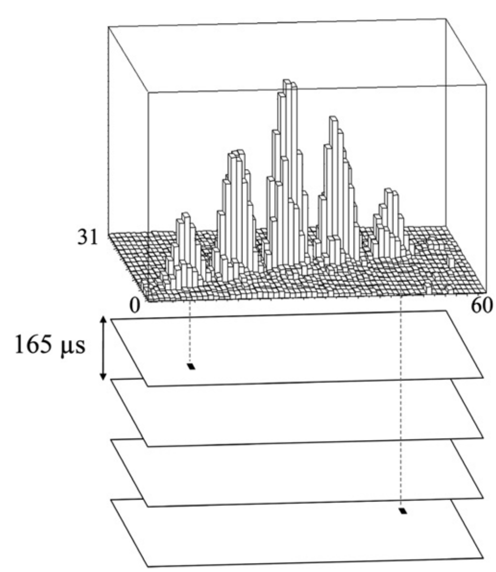

Fig. 2. Pictorial view of the stack of frames collected in a typical run.

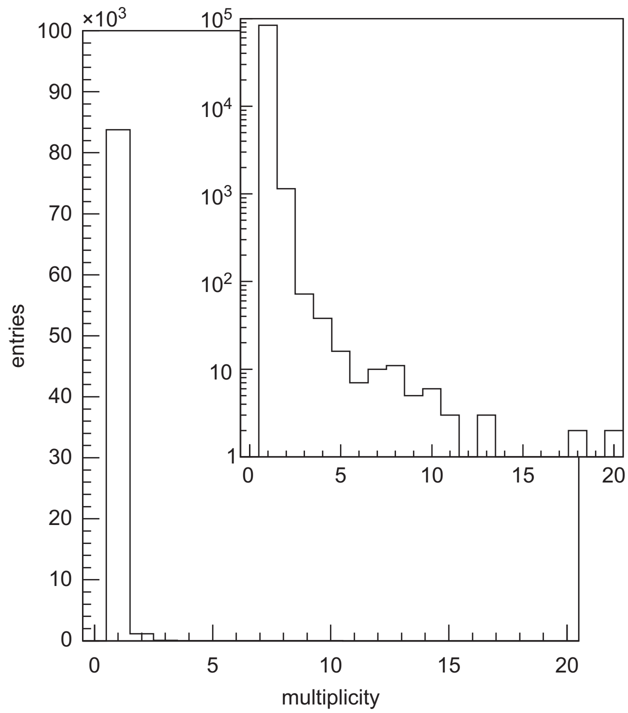

Fig. 3. Multiplicity distribution of hit pixels in the frames. The inset reports the same data on a logarithmic scale.

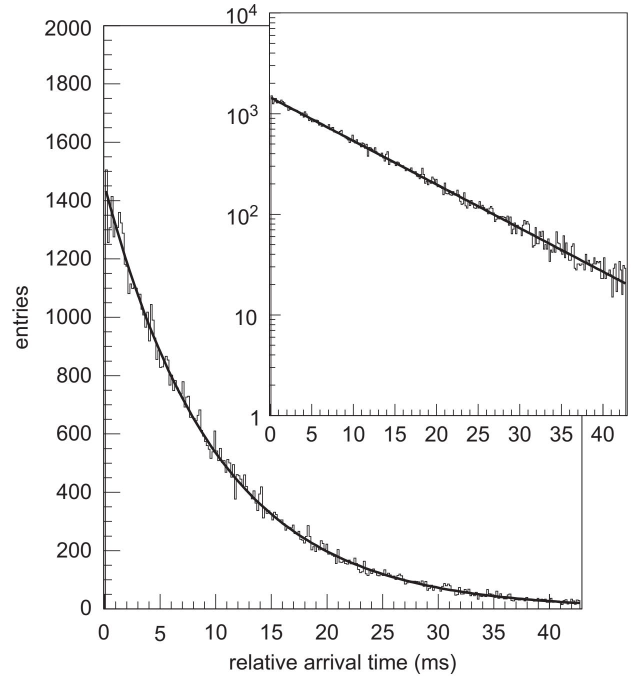

Fig. 4. Distribution of the time intervals between two consecutive non-empty events. The inset reports the same data on a logarithmic scale.

(actually a matrix of 128×32 pixels, in the figure being reported only its left half containing the central maximum) shows an one-hit event. Two successive empty frames are shown, while the fourth frame reports again one hit. The frame at the top of Fig. 2 reports the three dimensional histogram resulting from the superposition of 6000 frames. Electrons are accumulated in a few regions which correspond to the maxima of the two-slits interference pattern. In a typical run, 131k hit pixels were recorded in about 20 min, with a frame rate of 6.25 kfps.

In these conditions, the fraction of frames with electron multiplicity higher than one is about the one percent level, as confirmed by Fig. 3. From the measurement of the time interval which separates two adjacent non-empty frames, it is also possible to obtain the distribution of the interarrival time [21] of the electrons on the detector (Fig. 4). The fit of this distribution by an exponential function (and of its logarithm in the inset by a linear one) confirms that this is a Poisson process [22]. In particular, the obtained value for the slope is $-0.09975 \pm 0.00040\ \text{ms}^{-1}$, giving an average time interval between the detected electrons of 10.0 ms. When this number is compared with the time of flight within the electron microscope (9 ns), we see that the electron is completely read out before the next electron is emitted by the tungsten wire.

The coherence relation among the single electrons emerges when the different frames are added-up to form a single image. The interference scatter plot appears as expected from the interference of the two slits, placed at a certain distance, modulated by the diffraction due to their widths (Fig. 5(a)). The calibration of the camera length confirms that the spacing of the interference fringes is that expected and found in previous experiments [10]. Both the central diffraction maximum modulated by the interference fringes and the first secondary maximum at its right are visible. By averaging along the Y-axis (Fig. 5(b)) these latter are buried in the noise and masked by the presence of a malfunctioning pixel, giving a bright peak outside the interference pattern. Nonetheless, by fitting the Y average by means of the expression describing the interference of two partially coherent beams [10] it is possible to ascertain that the partial coherence of the illumination [23] has the value 0.6. It should be mentioned that similar images recorded after 20 min show the presence of a drift, so that these experimental conditions are right at the limit of the microscope stability.

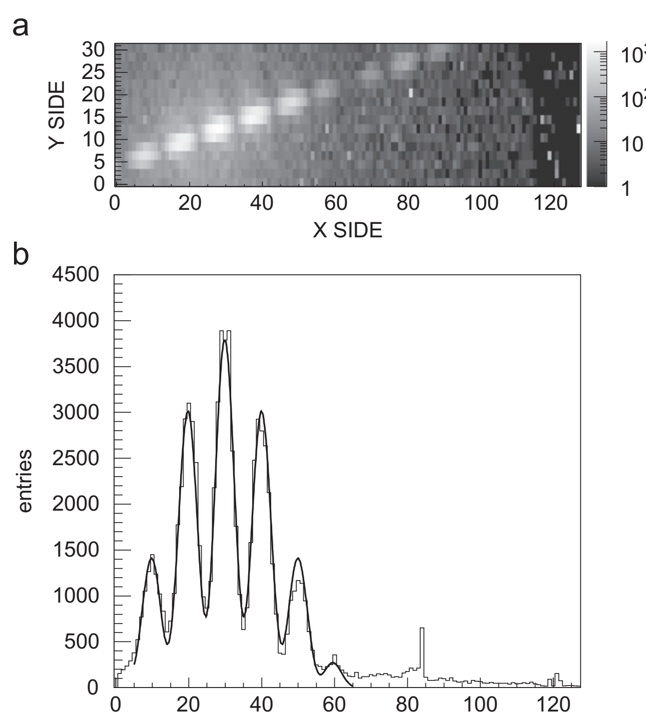

Fig. 5. Interference scatter plot obtained by adding-up the stack of frames (a), and its projection along the Y-axis (b).

4. Conclusions

By coupling modern specimen preparation methods and inserting a new detector in the electron microscope, we have realized the two-slits Young-Feynman experiment in the closest form to the original proposal, and the time distribution and the build-up of high statistic interference pattern of single electrons arriving on the screen have been obtained.

These results open interesting perspectives for future developments. The high statistics of single electrons will make possible to study the detailed properties of interference pattern formation which are connected to important tests of quantum mechanics. In the field of electron microscopy, the potential of our detector may open the way to reveal peculiar effects which take place both in static and time-dependent regime [24]. Last but not least, given the success of these preliminary experiments, work is in progress to assess more precisely the performance of the detector as well as to ascertain the potential of the electron microscope as an instrument for a detailed characterization of electronic chips. This represents an attractive opportunity since these tests are usually performed on particle beams at the accelerators with much higher costs.

Acknowledgements

We express our gratitude to SLIM5 Collaboration and INFN Bologna Section for their technical support. We wish to thank G. Balbi, R. Berti, A. Costa and S. Patuelli for their cooperation in developing the experiment and M. Pezzi and P. Mercati for their assistance in the experiment. We are also indebted to G.F. Missiroli for the useful discussions and enthusiastic encouragement.

References

[1] R.P. Feynman, R.B. Leighton, M.L. Sands, R.B. Leighton, M.L. Sands, The Feynman Lectures on Physics, Addison-Wesley Pub. Co, Reading, MA, 1963.

[2] G. Möllenstedt, H. Düker, Fresnelscher Interferenzversuch mit einem Biprisma für Elektronenwellen, Die Naturwissenschaften 42 (2) (1955) 41.

[3] G. Möllenstedt, H. Düker, Beobachtungen und Messungen an Biprisma-Interferenzen mit Elektronenwellen, Zeitschrift für Physik 145 (3) (1956) 377–397.

[4] G.F. Missiroli, G. Pozzi, U. Valdrè, Electron interferometry and interference electron microscopy, Journal of Physics E: Scientific Instruments 14 (6) (1981) 649–671.

[5] F. Hasselbach, Progress in electron- and ion-interferometry, Reports on Progress in Physics 73 (1) (2010) 1–43.

[6] C. Jönsson, Elektroneninterferenzen an mehreren künstlich hergestellten Feinspalten, Zeitschrift für Physik A Hadrons and Nuclei 161 (4) (1961) 454–474.

[7] C. Jönsson, Electron diffraction at multiple slits, American Journal of Physics 42 (1) (1974) 4–11.

[8] P.G. Merli, G.F. Missiroli, G. Pozzi, American Journal of Physics 44 (3) (1976) 306–307.

[9] A. Tonomura, J. Endo, T. Matsuda, T. Kawasaki, H. Ezawa, American Journal of Physics 57 (2) (1989) 117–120.

[10] S. Frabboni, G.C. Gazzadi, G. Pozzi, Nanofabrication and the realization of Feynman's two-slit experiment, Applied Physics Letters 93 (7) (2008) 073108-3.

[11] S. Frabboni, C. Frigeri, G.C. Gazzadi, G. Pozzi, Four slits interference and diffraction experiments, Ultramicroscopy 110 (5) (2010) 483–487.

[12] G. Deptuch, A. Besson, P. Rehak, M. Szelezniak, J. Wall, M. Winter, Y. Zhu, Direct electron imaging in electron microscopy with monolithic active pixel sensors, Ultramicroscopy 107 (8) (2007) 674–684.

[13] M. Battaglia, D. Contarato, P. Denes, D. Doering, P. Giubilato, T.S. Kim, S. Mattiazzo, V. Radmilovic, S. Zalusky, A rad-hard CMOS active pixel sensor for electron microscopy, Nuclear Instruments and Methods in Physics Research Section A: Accelerators, Spectrometers, Detectors and Associated Equipment 598 (2) (2009) 642–649.

[14] A. Gabrielli, G. Batignani, S. Bettarini, F. Bosi, G. Calderini, R. Cenci, M. Dell'Orso, F. Forti, P. Giannetti, M.A. Giorgi, A. Lusiani, G. Marchiori, F. Morsani, N. Neri, E. Paoloni, G. Rizzo, J. Walsh, C. Andreoli, L. Gaioni, E. Pozzati, L. Ratti, V. Speziali, M. Manghisoni, V. Re, G. Traversi, M. Bomben, L. Bosisio, G. Giacomini, L. Lanceri, I. Rachevskaia, L. Vitale, G.F. Dalla Betta, G. Soncini, G. Fontana, L. Pancheri, G. Verzellesi, D. Gamba, G. Giraudo, P. Mereu, R. Di Sipio, M. Bruschi, B. Giacobbe, F. Giorgi, C. Sbarra, N. Semprini, R. Spighi, S. Valentinetti, M. Villa, A. Zoccoli, A 4096-pixel MAPS device with on-chip data sparsification, Nuclear Instruments and Methods in Physics Research Section A: Accelerators, Spectrometers, Detectors and Associated Equipment 604 (1–2) (2009) 408–411.

[15] G. Rizzo, C. Avanzini, G. Batignani, S. Bettarini, F. Bosi, G. Calderini, M. Ceccanti, R. Cenci, A. Cervelli, F. Crescioli, M. Dell'Orso, F. Forti, P. Giannetti, M.A. Giorgi, A. Lusiani, S. Gregucci, P. Mammini, G. Marchiori, M. Massa, F. Morsani, N. Neri, E. Paoloni, M. Piendibene, A. Profeti, L. Sartori, J. Walsh, E. Yurtsev, M. Manghisoni, V. Re, G. Traversi, M. Bruschi, R. Di Sipio, B. Giacobbe, A. Gabrielli, F. Giorgi, G. Pellegrini, C. Sbarra, N. Semprini, R. Spighi, S. Valentinetti, M. Villa, A. Zoccoli, M. Citterio, V. Liberali, F. Palombo, C. Andreoli, L. Gaioni, E. Pozzati, L. Ratti, V. Speziali, D. Gamba, G. Giraudo, P. Mereu, G.F. Dalla Betta, G. Soncini, G. Fontana, M. Bomben, L. Bosisio, P. Cristaudo, G. Giacomini, D. Jugovaz, L. Lanceri, I. Rashevskaya, L. Vitale, G. Venier, The SuperB silicon vertex tracker, Nuclear Instruments and Methods in Physics Research Section A: Accelerators, Spectrometers, Detectors and Associated Equipment 617 (1–3) (2010) 585–587.

[16] S. Bettarini, L. Ratti, G. Rizzo, M. Villa, L. Vitale, J. Walsh, C. Avanzini, G. Batignani, F. Bosi, M. Ceccanti, R. Cenci, A. Cervelli, F. Crescioli, M. Dell'Orso, F. Forti, P. Giannetti, M.A. Giorgi, A. Lusiani, S. Gregucci, P. Mammini, G. Marchiori, M. Massa, F. Morsani, N. Neri, E. Paoloni, M. Piendibene, A. Profeti, L. Sartori, E. Yurtsev, L. Gaioni, V. Speziali, M. Bruschi, R. Di Sipio, L. Fabbri, B. Giacobbe, A. Gabrielli, F. Giorgi, G. Pellegrini, C. Sbarra, N. Semprini, R. Spighi, S. Valentinetti, A. Zoccoli, M. Bomben, L. Bosisio, P. Cristaudo, G. Giacomini, D. Jugovaz, L. Lanceri, I. Rashevskaya, G. Venier, M. Manghisoni, V. Re, G. Traversi, D. Gamba, G. Giraudo, P. Mereu, G.F. Dalla Betta, G. Soncini, G. Fontana, The SLIM5 low mass silicon tracker demonstrator, Nuclear Instruments and Methods in Physics Research Section A: Accelerators, Spectrometers, Detectors and Associated Equipment 623 (3) (2010) 942–953.

[17] F. Forti, C. Avanzini, G. Batignani, S. Bettarini, F. Bosi, G. Calderini, M. Ceccanti, R. Cenci, A. Cervelli, F. Crescioli, M. Dell'Orso, P. Giannetti, M.A. Giorgi, A. Lusiani, S. Gregucci, P. Mammini, G. Marchiori, M. Massa, F. Morsani, N. Neri, E. Paoloni, M. Piendibene, A. Profeti, G. Rizzo, L. Sartori, J. Walsh, E. Yurtsev, M. Manghisoni, V. Re, G. Traversi, M. Bruschi, R. Di Sipio, B. Giacobbe, A. Gabrielli, F. Giorgi, G. Pellegrini, C. Sbarra, N. Semprini, R. Spighi, S. Valentinetti, M. Villa, A. Zoccoli, M. Citterio, V. Liberali, F. Palombo, C. Andreoli, L. Gaioni, E. Pozzati, L. Ratti, V. Speziali, D. Gamba, G. Giraudo, P. Mereu, G.F. Dalla Betta, G. Soncini, G. Fontana, M. Bomben, L. Bosisio, P. Cristaudo, G. Giacomini, D. Jugovaz, L. Lanceri, I. Rashevskaya, L. Vitale, G. Venier, The SuperB silicon vertex tracker, Nuclear Instruments and Methods in Physics Research Section A: Accelerators, Spectrometers, Detectors and Associated Equipment 636 (1, Supplement 1) (2011) S168–S172.

[18] R.P. Crease, The most beautiful experiment, Physics World 15 (9) (2002) 19–20.

[19] R.P. Crease, The Prism and the Pendulum: The Ten Most Beautiful Experiments in Science, Random House, New York, 2003.

[20] R.R. Meyer, A.I. Kirkland, R.E. Dunin-Borkowski, J.L. Hutchison, Experimental characterisation of CCD cameras for HREM at 300 kV, Ultramicroscopy 85 (1) (2000) 9–13.

[21] S.M. Ross, Stochastic Processes, second ed., Wiley, New York, 1996.

[22] F.A. Haight, Handbook of the Poisson Distribution, Operations Research Society of America, Publications in Operations Research, vol. 11, Wiley, New York, 1967.

[23] M. Born, E. Wolf, Principles of Optics: Electromagnetic Theory of Propagation, Interference and Diffraction of Light, fourth ed., Pergamon Press, Oxford, 1969.

[24] A.H. Zewail, Four-dimensional electron microscopy, Science 328 (5975) (2010) 187–193.